On the diurnal ranges of Sea Surface Temperature (SST) in the north Indian Ocean

S S C Shenoi[1,3,*], N Nasnodkar[1], G Rajesh[2], K Jossia Joseph[2], I Suresh[1] and A M Almeida[1]

[1]*National Institute of Oceanography (Council of Scientific and Industrial Research), Dona Paula, Goa 403 004, India.*
[2]*National Institute of Ocean Technology (Ministry of Earth Sciences), Pallikarani, Chennai 600 100, India.*
[3]*Present address: Indian National Centre for Ocean Information Services (Ministry of Earth Sciences), Hyderabad, India.*
[*]*e-mail: shenoi@incois.gov.in*

This paper describes the variability in the diurnal range of SST in the north Indian Ocean using *in situ* measurements and tests the suitability of simple regression models in estimating the diurnal range. SST measurements obtained from 1556 drifting and 25 moored buoys were used to determine the diurnal range of SSTs. The magnitude of diurnal range of SST was highest in spring and lowest in summer monsoon. Except in spring, nearly 75–80% of the observations reported diurnal range below 0.5°C. The distributions of the magnitudes of diurnal warming across the three basins of north Indian Ocean (Arabian Sea, Bay of Bengal and Equatorial Indian Ocean) were similar except for the differences between the Arabian Sea and the other two basins during November–February (winter monsoon) and May. The magnitude of diurnal warming that depended on the location of temperature sensor below the water level varied with seasons. In spring, the magnitude of diurnal warming diminished drastically with the increase in the depth of temperature sensor. The diurnal range estimated using the drifting buoy data was higher than the diurnal range estimated using moored buoys fitted with temperature sensors at greater depths.

A simple regression model based on the peak solar radiation and average wind speed was good enough to estimate the diurnal range of SST at $\sim$1.0 m in the north Indian Ocean during most of the seasons except under low wind-high solar radiation conditions that occur mostly during spring. The additional information on the rate of precipitation is found to be redundant for the estimation of the magnitude of diurnal warming at those depths.

1. Introduction

The variability of sea surface temperature (SST) is widely studied due to its large impact on ocean–atmosphere interaction. Kawai and Wada (2007) provides an excellent review on the importance of the diurnal variability of SST on air–sea interaction. Diurnal variations in the SST affect longer time-scale variability events such as the MJO (Madden–Julian Oscillation) (Shinoda 2005) and ENSO (El Niño Southern Oscillation) (Solomon and Jin 2005). The diurnal change in SST has also been examined to study the possible feedbacks on the atmosphere (Clayson and Chen 2002; Bernie *et al* 2007). Solar heating of the sea surface in low-wind conditions can lead to the development of a stable warm layer of a few meters thickness at the surface. In the tropics, the diurnal warming in SSTs can have a significant magnitude of up to 3°C or more under calm and clear conditions (e.g., Yokoyama *et al* 1995; Fairall *et al* 1996; Minnett 2003). Since the SST

Keywords. Sea surface temperature; diurnal range; Indian Ocean; drifting buoys; moored buoys; data analysis; oceanography; monsoons.

J. Earth Syst. Sci. **118**, No. 5, October 2009, pp. 483–496

retrievals by satellites are of this thin surface layer, the diurnal warming effect strongly influences the measurements. The recent studies, using the data from satellite-based microwave and infrared sensors, indicated that a simple model of diurnal warming as a function of local time, wind speed and solar radiation can account for most of the diurnal warming (Gentemann *et al* 2003; Stuart–Menteth *et al* 2003). Stuart–Menteth *et al* (2003) also reported that the exclusion of diurnal cycle caused by the diurnal warming would introduce errors in the radiance assimilation in numerical weather prediction models leading to inaccuracies in the estimation of air–sea fluxes, and SST itself.

Due to the limitations in the coverage of *in situ* measurements of diurnal SSTs, a number of studies have exploited the satellite data (see e.g., Stramma *et al* 1986; Kawai and Kawamura 2002; Gentemann *et al* 2003; Stuart–Menteth *et al* 2003, etc.) to study its variability. However, due to the constraints in the pass time of satellites, their ability to sample the diurnal cycle is limited. To overcome this constraint, Clayson and Weitlich (2007) used the peak shortwave solar radiation determined from International Satellite Cloud Climatology Project (ISCCP) data and the daily averaged wind speed determined from Special Sensor Microwave Imager (SSM/I) data as inputs to a regression model (Webster *et al* 1996) to determine the diurnal warming range. Several reports are available from Pacific (Webster *et al* 1996) and Atlantic (Cornillon and Stramma 1985; Stramma *et al* 1986; Price *et al* 1987) Oceans on the *in situ* measurements of diurnal cycles in SST. However, such reports on the *in situ* measurements of diurnal SST are lacking in the Indian Ocean, except for the global climatology of diurnal warming produced by Kennedy *et al* (2007) using drifting buoy observations. The Indian Ocean exhibits a large annual cycle in SST owing to reversing monsoonal winds and the associated air–sea interaction processes, and therefore, it deserves more attention than was accorded in the global climatology of Kennedy *et al* (2007). Modelling studies of McCreary *et al* (2001) demonstrated the importance of diurnal cycle in the estimation of phytoplankton biomass in the Arabian Sea. The *in situ* measurements at a site in the Arabian Sea showed that the maximum amplitude of diurnal cycle in SST occurs during the spring inter-monsoon (March–April), when the mixed layer depth is at its minimum, and the minimum ($<0.1^\circ$C) amplitude occurs during the summer monsoon, when the winds are highest (Weller *et al* 2002). Due to the averaging processes in the climatology (e.g., Kennedy *et al* 2007), an average picture emerges, but not the magnitude of variability experienced during the diurnal warming events. Hence, this study aims at providing a quantitative description of the magnitude of diurnal range of SST over the north Indian Ocean region by retaining the high variability experienced by it. This study also examines the suitability of simple regression models in reproducing the diurnal range of SST in the north Indian Ocean and examines the conditions under which the simple models fail to reproduce the diurnal SST accurately.

Section 2 describes the *in situ* SST measurements used for this study. Section 3 presents and discusses the results based on spatial and seasonal variability of diurnal range using the SST data obtained from drifting and moored buoys and also, examines the suitability of simple models in reproducing the peak diurnal warming based on wind speed and solar radiation. Section 4 summarises the results.

2. Data

Usually the diurnal peak of SST is observed between pre-noon and late afternoon. Price *et al* (1986) reported that the surface warming typically peaks around 14:30 h local solar time, but with considerable scatter. In some cases the warming peaked before noon. Yokoyama *et al* (1995) and Zeng *et al* (1999) reported that the peak warming occurred a couple of hours after midday. In the present case, most of the observations reported SST maxima occurring during 13:00–16:00 h and the minima occurring during 04:00–07:00 h. Widening the time windows by an hour or two only helped in the inclusion of a few more observations; but their numbers were negligible. Hence, in this study, the magnitude of the range of diurnal SST is defined as the difference between the afternoon maximum value of SST during the time window 13:00–16:00 h and the morning minimum during the time window 04:00–07:00 h. Henceforth, we denote this difference in afternoon and morning SST as ΔSST. We have used five major sets of *in situ* measurements to describe the magnitude of diurnal SST range (table 1). The dataset includes the data from 1556 drifting buoys and 25 moored buoys. The drifting buoy data spans over a period of 19 years during 1989 to 2007. It includes the data from the buoys deployed by National Institute of Oceanography (NIO), India and the data archived at Global Drifter Data Centre in AOML (Atlantic Oceanographic and Meteorological Laboratories), USA. The data from moored buoys consist of the data from the WHOI (Woods Hole Oceanographic Institution) mooring in the west-central Arabian Sea (Weller *et al* 1998), the RAMA (The Research Moored Array for African–Asian–Australian Monsoon Analysis and Prediction) and the TRITON

Table 1. *Details of data used.*

Source	Type	No. of buoys	Duration	Location	Parameters	Sampling interval	Depth of SST sensor (m)
NIO	Drifting	173	January 1992–December 2007	Spread over north IO	SST	1 h	0.20
AOML	Drifting	1383	January 1989–December 2006	Spread over north IO	SST	1 h	0.20
WHOI	Moored	1	16 October 1994–10 October 1995	Western AS	SST, wind speed, solar radiation, precipitation rate	7.5 min	0.92
RAMA	Moored	1	10 November 2004–26 March 2006	EIO	SST, wind speed, solar radiation	10 min	1.00
TRITON	Moored	1	23 October 2001–31 July 2007	EIO	SST, wind speed, solar radiation	1 h	1.50
NDBP	Moored	22	August 1997–December 2006	Seas around India	SST, wind speed	3 h	3.0

(Triangle Trans-Ocean buoy Network) moorings in the eastern Equatorial Indian Ocean and the 22 buoys moored in the seas around India by the National Data Buoy Programme (NDBP) of National Institute of Ocean Technology, India.

It is important to note that the location of SST sensors on the buoys used for this analysis were not all at the same depths (table 1). Hence, the magnitudes of SST reported by the sensors attached to different types of buoys might vary from one to another due to the sharp gradients in the temperature within the upper few meters of water column (see Kawai and Wada 2007 and references therein). Considering the differences in the SST measured at different levels, the Global Ocean Data Assimilation Experiment (GODAE) High-Resolution SST Pilot Project (GHRSST-PP) science team categorised them under five kinds of SSTs (Donlon and the GHRSST-PP science team 2005). They are, interface SST, skin SST, sub-skin SST, SST at depth and foundation SST. The satellite based measurements report the 'skin SST' (at a depth of few micrometers) and most of the *in situ* measurements report the 'SST at depth' (at depths of few cm to 1.0–5.0 m). The SST at depth is also simply referred as 'bulk' SST. Following this categorisation, the SSTs used here may be considered as 'SST at depth'; where the depth varies from 0.20 m (for drifters) to 0.92–3.0 m (for moored buoys).

The drifting buoy data have a wider spatial and temporal distribution than the other three datasets, which are measurements at fixed locations over a limited period. Together, more than one million (1070,000) SST measurements from drifting buoys were available from the Indian Ocean north of 10°S during 1989–2007. However, no auxiliary measurements of wind speed, solar radiation and precipitation were available with the drifting buoy SSTs. The SST data obtained from drifting as well as the moored buoys were quality-controlled following Hansen and Poulain (1996).

The daily time series of ΔSST for each buoy was prepared by subtracting the minimum SST value within the morning time window from the maximum SST value within the afternoon time window. Unlike the moored buoys, the drifting buoys shifted their locations between morning and afternoon measurements. Hence, the SST values obtained from drifting buoys are not necessarily from the same location. However, considering the slow movement of drifting buoys, the SSTs reported in the morning and afternoon windows are accepted as the SSTs from the same location. The distance moved by the buoys used for this analysis was less than 30 km in 95% of the cases. The maximum distance drifted by any buoy between the morning and afternoon measurement of SST did not exceed 75 km.

Since the monsoonal climate controls the air–sea interaction processes over the north Indian Ocean, the data from all sources were grouped under five different seasons, namely, winter monsoon (November–February), summer monsoon (June–September), spring (March–April), and two inter-monsoonal months, May and October. May represents the conditions prior to the summer monsoon and October represents the inter-monsoonal period between summer and winter monsoon. To examine the variability of the magnitudes of ΔSST within a season, they were grouped in 0.2°C bins according to their magnitudes varying from −0.5°C to 2.1°C. The ΔSSTs that exceeded 2.1°C were grouped in the >2.1°C bin. The bin width of 0.2°C was chosen considering the measurement accuracy of temperature sensors attached to the drifting (0.1°C) and moored (0.002–0.005°C) buoys.

3. Results and discussions

3.1 *Spatial and seasonal variability of diurnal warming ranges*

The data from drifting buoys describe the spatial and seasonal variability of ΔSST effectively due to their spread in space and time. Figure 1 shows the distribution of ΔSST and the percentage of occurrences during various seasons in the north Indian Ocean as a whole, as well as in the Arabian Sea (AS; the region north of 6°N and west of 80°E), the Bay of Bengal (BB; the region north of 6°N and east of 80°E), and the Equatorial Indian Ocean (EIO; the region between 5°S and 6°N). The seasonwise number of observations in the sub-regions of the north Indian Ocean and the related statistics are shown in table 2. During all seasons, the maximum number of ΔSST values in the north Indian Ocean fell in the range of 0.1°–0.5°C. The percentage of ΔSSTs in the 0.1°–0.5°C range was lowest in spring (50%) and highest in summer monsoon (72%). Most of the higher ΔSSTs (>0.5°C), however, occurred during spring. During this season, 47% of the ΔSST values were higher than 0.5°C. About 3% of them even exceeded 2.1°C (figure 1-c1). On the other hand, the percentage of ΔSST exceeding 0.5°C was 25% in October and May (figure 1-f1 and d1). During the summer monsoon, only 14% of ΔSST values exceeded 0.5°C (figure 1-e1); hardly any value exceeded 1.1°C.

Annually, for the AS region, 78% of the ΔSST values were <0.5°C and the rest were >0.5°C (figure 1-a2). The corresponding percentages for the BB and EIO regions were 73 and 75 respectively (figure 1-a3 and a4). The highest percentage of ΔSST in the range of 0.1°–0.5°C as well as in the range of −0.5° to 0.1°C occurred in summer (figure 1-e1–e4) and winter monsoons (figure 1-b2–b4) and the highest percentage of ΔSST in the range of 0.5°–1.1°C and above occurred in spring (figure 1-c2–c4) in all three regions.

To check whether the distributions of ΔSST are similar at any two regions during a season, we have used the Cramér-von-Mises test. The test hypothesis was that the two samples came from the same population (Anderson 1962). The p-values (table 3) estimated using this test suggest that the differences between the distributions of ΔSST in the three regions are similar except for the difference in the distribution of ΔSST in the AS and the BB during winter monsoon and between the AS and BB as well as EIO in May. Hence, the differences in the diurnal warming magnitudes are similar over the north Indian Ocean except for the differences during some seasons. The lack of significant regional differences in the diurnal warming magnitudes over the north Indian Ocean are, however, different from the observations of Kawai and Wada (2007) based on satellite SSTs and the modelled diurnal SSTs of Bernie *et al* (2007). Both studies showed greater diurnal warming in the EIO except in spring. The diurnal warming reported in Kawai and Wada (2007) reflects the 'SST_{skin}' and the modelled SST (1.0 m) in Bernie *et al* (2007); whereas our observations correspond to the 'SST_{depth}' (at ∼0.20 m). As mentioned earlier, the diurnal warming magnitudes differ with depth (Fairall *et al* 1996; Clayson and Chen 2002; Kawai and Wada 2007). The magnitudes of diurnal warming differing with depth also could be a reason for the difference in the spatial variability in our analysis and that in Kawai and Wada (2007) and Bernie *et al* (2007). Another difference between their analysis and our analysis is that we looked at the distributions of ΔSST aggregated over the three basins whereas their analysis looked at point averages of ΔSST.

Figure 2 shows the locations of moored buoys used for the analysis and figure 3 shows the time series of ΔSST obtained from some of them. In general, the ΔSST estimated from the NDBP buoys showed low values (figure 3b–f) compared to those obtained from WHOI (figure 3a), TRITON (figure 3h) and RAMA (figure 3g) during spring. Specifically, the ΔSST at DS1 (figure 3b) and DS3 (figure 3d) buoys located in the offshore regions in AS and BB showed too low values. The probable reasons for the lower ΔSST estimates reported by the NDBP buoy are discussed later in this section.

At the WHOI buoy in the AS, ΔSST was lowest (<0.5°C) during summer and winter monsoons (figure 3a). Maximum number of warm ΔSST (>0.5°C) occurred during February–April;

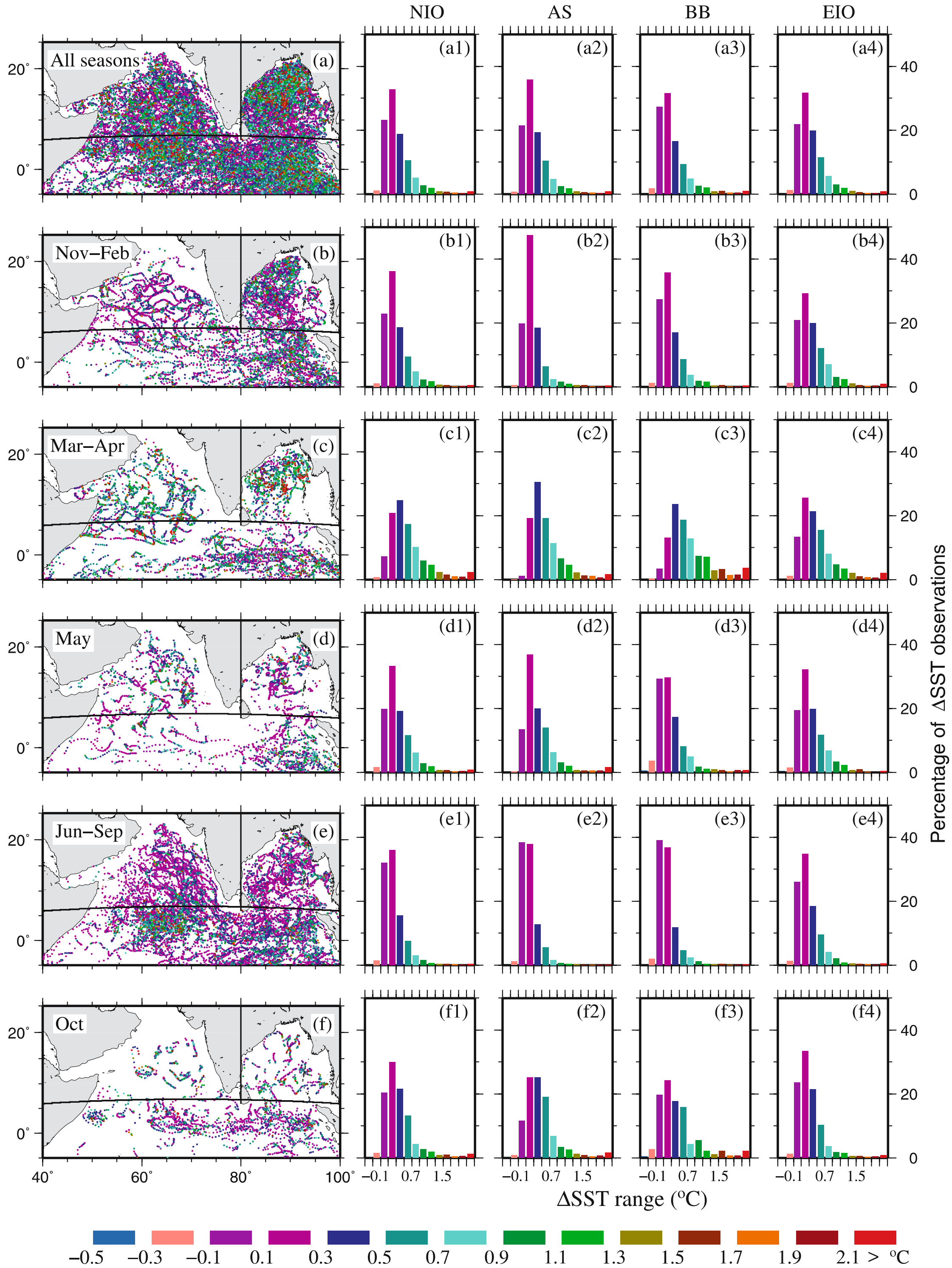

Figure 1. Spatial (maps) and seasonal (bar graphs) distribution of the magnitude of diurnal range of SST (ΔSST) in the north Indian Ocean estimated using the data obtained from drifting buoys. Data from 1556 drifters were used to estimate the ΔSST. The dot in the map indicates the locations at which the ΔSST was estimated using the morning and afternoon SSTs and the colour indicates the magnitude of ΔSST. ΔSST values exceeding 2.1°C are also included in >2.1°C bin.

the amplitude even exceeded 2.0°C on a few occasions. As with the distribution of ΔSSTs estimated from the drifter observations, most of the ΔSST values were below 0.5°C during all seasons. During the summer monsoon, 98% of the ΔSST values were below 0.5°C (figure 4-e2). During this season, about 10% of them showed negative ΔSST values indicating cooling in the afternoon. The cooling in the afternoon could have been caused due to the increased cloud cover and increased wind

Table 2. *Seasonwise statistics of ΔSST observations obtained from the drifting buoys deployed in the north Indian Ocean (north IO) during 1992–2007. The north IO was divided into three regions namely Arabian Sea (AS, the region north of 6°N and west of 80°E), Bay of Bengal (BB, the region north of 6°N and east of 80°E) and Equatorial Indian Ocean (EIO, the region between 5°S and 6°N) to examine the regional distribution of ΔSST. Data from 1556 drifting buoys were used. Difference between the minimum SST during 04:00–07:00 h and the maximum SST during 13:00–16:00 h were considered as the magnitude of diurnal warming, ΔSST.*

		North IO	AS	BB	EIO
All Seasons	No. of observations	25266	6859	6378	12029
	Minimum	−1.84	−0.95	−1.19	−1.84
	Maximum	4.08	3.70	4.08	3.92
	Mean	0.36	0.36	0.34	0.37
	Median	0.25	0.25	0.21	0.28
	Standard deviation	0.41	0.39	0.43	0.40
November–February (Winter)	No. of observations	7132	1703	2657	2772
	Minimum	−1.19	−0.44	−1.19	−0.88
	Maximum	3.70	3.70	2.56	3.28
	Mean	0.33	0.30	0.28	0.39
	Median	0.24	0.20	0.17	0.30
	Standard deviation	0.36	0.32	0.33	0.40
March–April (Spring)	No. of observations	4417	1490	887	2040
	Minimum	−0.80	−0.32	−0.20	−0.80
	Maximum	4.08	3.36	4.08	3.76
	Mean	0.60	0.62	0.75	0.53
	Median	0.48	0.50	0.56	0.40
	Standard deviation	0.51	0.45	0.57	0.51
May (Inter-monsoon)	No. of observations	2617	912	636	1069
	Minimum	−0.60	−0.17	−0.60	−0.48
	Maximum	3.12	3.12	2.36	2.29
	Mean	0.38	0.45	0.31	0.36
	Median	0.27	0.32	0.20	0.26
	Standard deviation	0.40	0.45	0.40	0.35
June–September (Summer)	No. of observations	9246	2379	1860	5007
	Minimum	−1.84	−0.56	−0.76	−1.84
	Maximum	3.92	2.15	3.90	3.92
	Mean	0.26	0.20	0.21	0.31
	Median	0.17	0.16	0.16	0.24
	Standard deviation	0.32	0.23	0.31	0.35
October (Inter-monsoon)	No. of observations	1854	375	338	1141
	Minimum	−1.02	−0.95	−0.48	−1.02
	Maximum	3.52	2.90	3.52	2.72
	Mean	0.39	0.48	0.47	0.33
	Median	0.30	0.36	0.32	0.25
	Standard deviation	0.43	0.47	0.54	0.36

speeds in the afternoons or due to the convective systems that often form during the summer monsoon. Highest number of ΔSST values above 0.5°C occurred in March–April (∼47%) following the low-wind speeds and high solar radiation that exist during spring. The percentage of ΔSSTs that exceeded 0.5°C during other seasons varied between 2% in the summer monsoon to 30% in May.

At the RAMA mooring in the EIO, ΔSST was lowest (<0.5°C) during June–August and in November–December. Maximum number of warm ΔSST (>0.5°C) occurred during February–April (figure 3g). The ΔSST distribution at this buoy appears to be similar to that at WHOI during summer monsoon and spring. However, during the winter monsoon, it is marginally warmer than that at WHOI. During spring, 30% of ΔSST exceeded 0.5°C (figure 4-c4). The percentage of warmer ΔSSTs (>0.5°C) during the other seasons varied from 9% in summer monsoon to 17% in winter monsoon (figure 4-e4, 4-b4).

Table 3. *Comparisons between the ΔSST distributions in AS, BB and EIO. p-values between two distributions (AS-BB, AS-EIO and BB-EIO) were estimated following Cramér-von-Mises test. The hypothesis was tested at 5% significance level. The p-values less than 0.05 indicate that the two distributions are significantly different. The significantly different pairs are underlined.*

	p-values		
Seasons	AS-BB	AS-EIO	BB-EIO
Winter (November–February)	<u>0.0320</u>	0.3951	0.0958
Spring (March–April)	0.4968	0.0884	0.1589
Inter-monsoon (May)	<u>0.0371</u>	<u>0.0057</u>	0.1998
Summer (June–September)	0.2403	0.7564	0.2242
Inter-monsoon (October)	0.2642	0.3398	0.8554

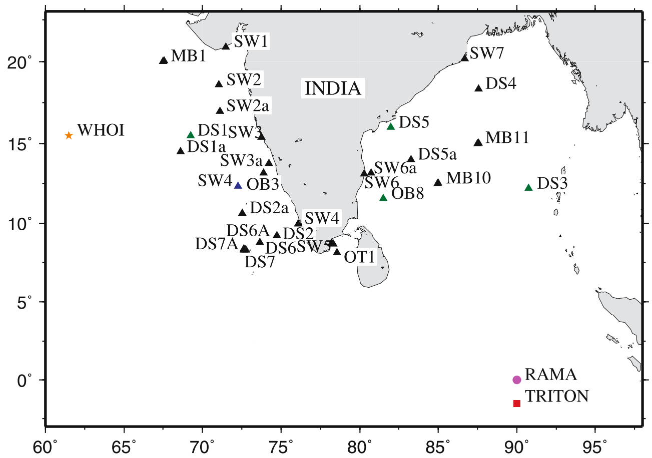

Figure 2. Locations of the moored buoys used. The moored buoys AN, DS, MB, OB, DS and SW belongs to NDBP programme (triangles). SST data obtained from these buoys (22 numbers) during August 1997 to December 2006 were used. The green triangles indicate the NDBP buoys used to construct figure 3. WHOI buoy was deployed and maintained (15 October 1994–10 October 1995) by R Weller of the Woods Hole Oceanographic Institute and TRITON buoy was deployed and maintained by Japan Marine Science and Technology Center. Data from the TRITON buoy deployed during 23 October 2001 to 31 July 2007 was used. RAMA mooring was deployed and maintained by PMEL (Pacific Marine and Environmental Laboratory, USA). Data for the period during 10 November 2004 to 26 March 2006 was used. The data from WHOI, RAMA and TRITON moorings were downloaded from the respective web sites and the data from the moored buoys around India were obtained from the data archive of NDBP.

At the TRITON buoy in the EIO, ΔSST was lowest (<0.5°C) during July–August and October (figure 3h). At this buoy also, the season-wise distribution of ΔSST was similar to that at the WHOI buoy in the AS (figure 4), but for one difference. At WHOI buoy, the largest number of ΔSST values having magnitudes less than 0.5°C occurred in the summer monsoon (98%), whereas at the TRITON buoy, the largest number of ΔSST values below 0.5°C occurred in October (∼95%). During the summer monsoon, 92% of ΔSSTs were below 0.5°C at TRITON buoy. During other seasons, that percentage varied from 72 in spring to 88 in May. The maximum number of ΔSST above 0.5°C (∼28%) occurred during spring (figure 4-c3).

The distribution of ΔSST over various ranges for the NDBP buoys is also similar to that at WHOI and TRITON, except for many negative ΔSSTs and for less warmer ΔSSTs in spring. During most of the seasons, about 25% of the ΔSST values were negative, the highest among all buoys. The maximum number of negative ΔSST values (∼35%) occurred during the summer monsoon. Similarly, the percentage of ΔSST exceeding 0.5°C too was comparatively low. Even during spring, less than 10% of the ΔSST values exceeded 0.5°C (figure 4-c5). However, similar to the ΔSST distributions at WHOI, RAMA and TRITON, the maximum number of ΔSST values fell in the range 0.0–0.5°C.

In general, the distribution of ΔSST over different ranges, estimated using the moored buoy SSTs (figure 4) is similar to that observed by the drifting buoys (figure 1). ΔSSTs exceeded 0.5°C more often during spring (figure 4-c1) than in any other season. Similarly, the cooler ΔSSTs (<0.5°C) more often existed during the summer monsoon; less than 10–14% of the ΔSSTs exceeded 0.5°C during the summer monsoon. In essence, the observations from the drifting as well as the moored buoys suggest that the diurnal warming magnitude over the north Indian Ocean is mostly less than 0.5°C during most of the seasons though the cases of higher magnitudes (>0.5°C) are also considerable. The highest number of higher magnitudes (ΔSST > 0.5°C) occurred in spring and highest number of lower magnitudes occurred during the summer monsoon.

The seasonality in the magnitudes of diurnal warming was also seen in the climatologies of Kennedy *et al* (2007) and Clayson and Weitlich (2007). Both climatologies used summer and winter

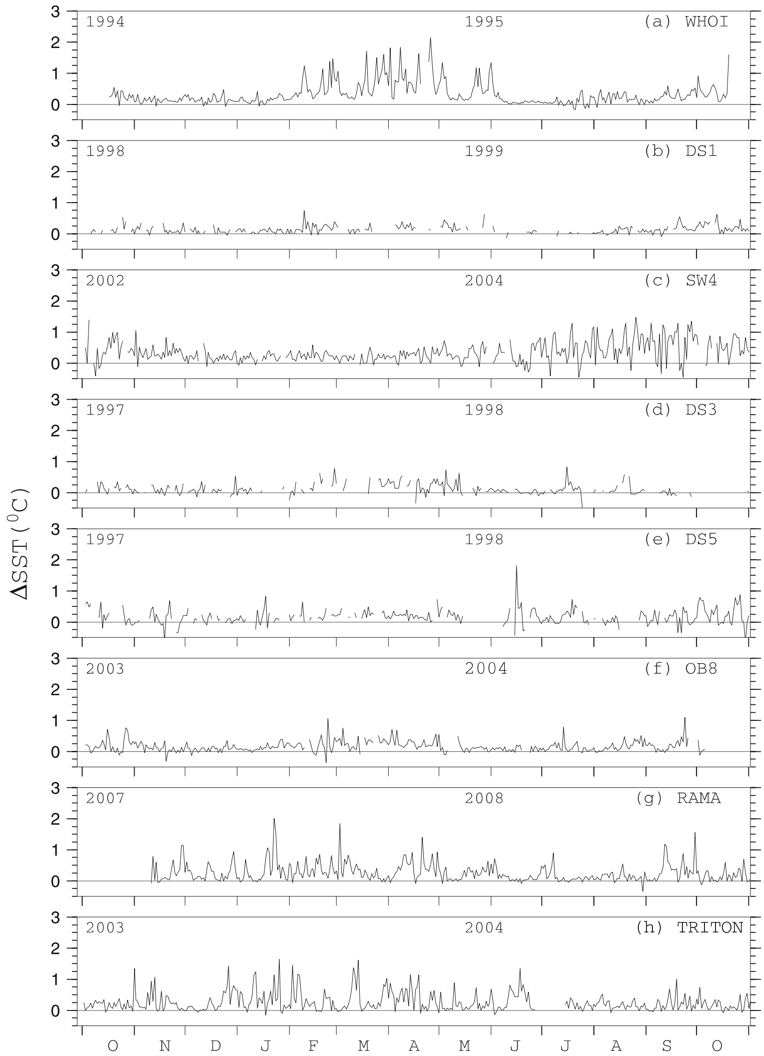

Figure 3. Time series of ΔSST estimated from the SST measured using some of the moored buoys. See figure 2 for the location of buoys. Note that the time series are for different years though the months are same (years are indicated in each panel).

monsoons to represent the extremes in the magnitudes of diurnal warming. Our analysis shows that the extremes in the magnitudes of diurnal warming exist between summer monsoon and spring rather than between summer and winter monsoons. The climatology of Kennedy *et al* (2007) showed warm ΔSSTs in EIO during summer and winter monsoons. The global maps of diurnal SST presented in Kawai and Wada (2007) also showed warm diurnal SST in EIO during spring and cooler diurnal SSTs in the summer monsoon in AS and BB. Our map (figure 1e) also showed warmer ΔSSTs in EIO than that in AS and BB during summer monsoon. But the statistical test (see table 3) did not suggest that the differences are significant at 95% confidence level. The magnitude of diurnal warming reported in those climatologies also did not exceed 0.5°C due to the averaging process associated with the production of climatology. The analysis presented here, however, suggests that the magnitudes of ΔSST exceed >0.5°C on large number of occasions. For example, in spring, 47% of the ΔSSTs exceeded 0.5°C, and in May and October, ∼25% of them exceeded 0.5°C.

The global maps of diurnal warming prepared using the satellite data indicated higher diurnal warming in spring over the north Indian Ocean compared to other seasons (Stuart–Menteth *et al* 2003; Kawai and Wada 2007). This is consistent with the analysis reported here based on the *in situ* measurement of SSTs using drifting buoys. The higher diurnal warming patch (> 0.5°C) over the central and eastern EIO in July (figure 1e) as well as the similar patches in the western EIO and BB in October (figure 1f) are consistent with the results reported in Stuart–Menteth *et al* (2003). However, the strong diurnal warming (>0.5°C) seen over the

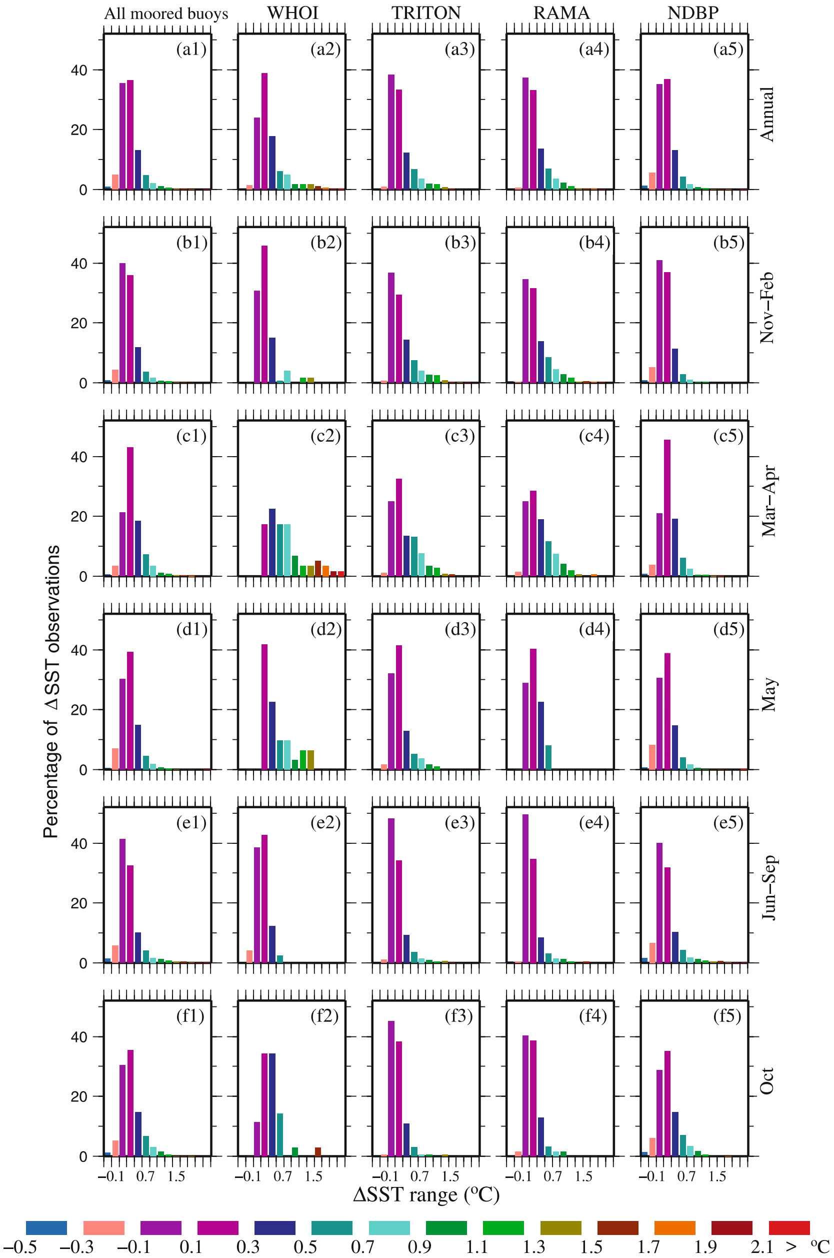

Figure 4. Bar charts showing the seasonal distribution of the range of ΔSST magnitudes estimated using the SST data obtained from WHOI, RAMA, TRITON and NDBP moored buoys. The buoywise ΔSST values are also shown. ΔSST values exceeded 2.1°C are included in the bin >2.1°C.

BB in July in Stuart–Menteth *et al* (2003) analysis is not seen in our analysis (figure 1e) or in the analysis of Kawai and Wada (2007) based on the microwave sensor based SSTs. The ΔSST values remained below 0.5°C in our analysis as well as in the analysis of Kawai and Wada (2007). The difference between the analysis of Stuart–Menteth *et al* (2003) and the results reported here may have arisen for two reasons. First, the satellite derived SST represents the skin SST, which is prone to higher diurnal warming than the *in situ* SST measured at 0.20 m. Kawai and Kawamura (2002) have reported twice-large diurnal magnitudes in skin SSTs than that measured at 1.5 m below the water level in the western Pacific. Second, during July, the sky over the BB is mostly cloudy and the satellite observations of SSTs using infrared sensors are prone to higher inaccuracies (Shenoi 1999; Sreejith and Shenoi 2002). Stuart–Menteth *et al* (2003) used the infrared-sensor-based SSTs to prepare the global maps of diurnal warming. In addition to the above, three other possibilities also exist:

(i) it could be that the six years covered by Stuart–Menteth analysis, the ΔSST really was higher;

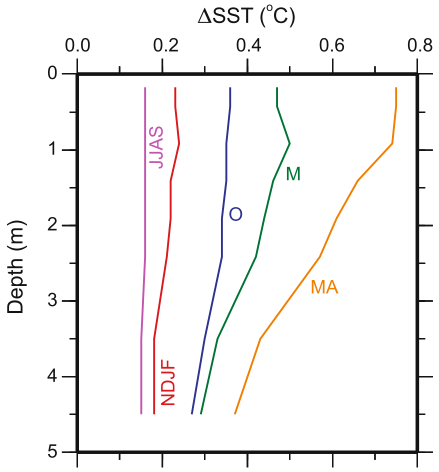

Figure 5. Variations in ΔSST with depth and seasons. Temperature measurements available from WHOI mooring at eight levels (0.17, 0.43, 0.92, 1.41, 1.91, 2.42, 3.50 and 4.50 m) were used.

(ii) we are comparing the distribution to a mean figure in which the instances of ΔSST exceeding 0.5°C are few (see the frequency map in figure 9 of Stuart–Menteth *et al* (2003), and

(iii) there could be a clear sky bias because drifters measure SST regardless of the weather, but infra-red sensors on board satellites can only measure SST when the skies are clear.

In general, the drifting buoys reported a higher percentage of warmer ΔSST values than that reported by moored buoys (figures 1 and 4, and also see figure 3). For example, the percentage of warmer ΔSST (>0.5°C), for each season was higher for drifters than that for moored buoys. Among the moored buoys also, the ΔSST estimates from WHOI buoy were warmer than those estimated from RAMA and TRITON. The ΔSST values were still cooler when they were estimated using the data from NDBP buoys (figure 3). As indicated earlier the SST sensor on the drifter was placed closer to the sea surface (0.20 m) than that on the moored buoys. The SST sensors of NDBP buoys were placed at 3.0 m below the water level and they were at 0.92 m, 1.0 m and 1.5 m respectively on WHOI, RAMA and TRITON buoys. Following the definitions of SST (Donlon and GHRSST-PP science team 2005), the SSTs reported here corresponds to 'SST at depth'. The SST from the drifters represents $\mathrm{SST}_{0.20\,\mathrm{m}}$ and the SST from NDBP buoy represents $\mathrm{SST}_{3.0\,\mathrm{m}}$. Due to the sharp temperature gradients, normally, the $\mathrm{SST}_{3.0\,\mathrm{m}}$ will be cooler than $\mathrm{SST}_{0.20\,\mathrm{m}}$. As a consequence, the magnitude of diurnal warming at deeper depth also will be lower than that at the shallower depth. The diminishing magnitude of diurnal warming with the increase in depth observed here are consistent with the reports from western Pacific (Fairall *et al* 1996; Clayson and Chen 2002). No such reports, however, are available for the north Indian Ocean region.

Hence, to further investigate the variability of diurnal warming with depth, we have analysed the temperature measurements available at eight levels (0.17, 0.43, 0.92, 1.41, 1.91, 2.40, 3.50 and 4.50 m) from WHOI mooring. The ΔSST within the 4.5 m layer not only varied with depth but also with seasons (figure 5). The depth dependence of ΔSST is highest during spring and lowest during summer monsoon when the strong monsoonal wind mixes the upper water column. The ΔSST during winter monsoon also is low owing to the convective mixing of the upper water column. During spring, the ΔSST dropped from 0.75°C at 0.17 m to 0.37°C at 4.5 m; during the intermonsoonal month of May, the ΔSST dropped from 0.48°C to 0.3°C. Hence, in the north Indian Ocean, the decrease in the magnitude of ΔSST with increasing depth is highly seasonal.

3.2 *Suitability of empirical models for the estimation of ΔSST in the north Indian Ocean*

Having described and discussed the distribution of ΔSST over the north Indian Ocean, we have also examined the suitability of the empirical models suggested by Webster *et al* (1996) and Kawai and Kawamura (2002) to estimate ΔSST. The model of Webster *et al* (1996) used three parameters – average wind speed (U), daily peak solar radiation (PS), and average precipitation rate (P), while the model of Kawai and Kawamura (2002) used only the first two parameters. Both models were developed using data from the western Pacific.

The regression model of Webster *et al* (1996) has the form

$$\Delta\mathrm{SST} = a(PS) + b(P) + c[\ln(U)] + d(PS)[\ln(U)] + e(U) + f, \qquad (1)$$

where a, b, c, d, e and f are the regression coefficients. The model proposed by Kawai and Kawamura (2002) has the form

$$\Delta\mathrm{SST} = a(PS)^2 + c[\ln(U)] + d(PS)^2[\ln(U)] + f. \qquad (2)$$

The data assembled from drifting buoys do not have information on the parameters used in the

Table 4. *Regression coefficients for the estimation of ΔSST. Data from WHOI, RAMA and TRITON moorings were used.*

Equation	Data	*a*	*b*	*c*	*d*	*e*	*f*
1	WHOI	3.34×10^{-3}	-2.75×10^{-1}	3.35×10^{-1}	-1.56×10^{-3}	1.19×10^{-1}	-1.63
2	WHOI	3.00×10^{-6}	–	1.10×10^{0}	-0.20×10^{-6}	–	-1.94×10^{0}
2	RAMA	1.00×10^{-6}	–	-3.33×10^{-2}	-0.01×10^{-6}	–	0.11×10^{0}
2	TRITON	1.00×10^{-6}	–	-1.26×10^{-1}	-0.001×10^{-6}	–	0.28×10^{0}

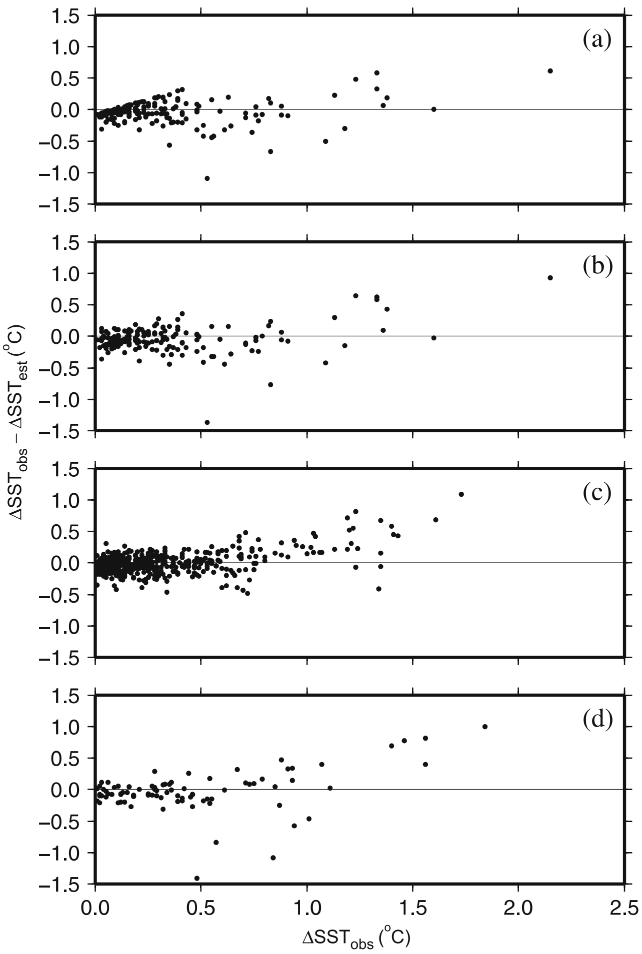

Figure 6. The errors in the estimation of ΔSST using the regression models proposed by **(a)** Webster *et al* 1996 (equation 1), **(b)** Kawai and Kawamura 2002 (equation 2). Both models were applied on the data from WHOI moored buoy. (**c** and **d**) Same as above, but the Kawai and Kawamura model applied on the data from TRITON and RAMA moored buoys respectively.

above equations. Similarly, the data assembled from the data archives of NDBP also do not have the information on solar radiation. The WHOI mooring provides data on wind speed, solar (short wave) radiation, and precipitation, whereas the TRITON and RAMA moorings provide data on wind speed and solar radiation only. Hence, only the WHOI data were used to test both models; the data from, the TRITON and RAMA moorings were used to test the model proposed by Kawai and Kawamura (2002). For independent evaluation of the models, one half of the dataset, selected randomly, was used to estimate the regression coefficients (table 4) and the other half was used for the evaluation of regression coefficients.

The differences between the observed and the model ΔSSTs are shown in figure 6. Only the data that was not included for the estimation of regression coefficients was used in figure 6. The model of Webster *et al* (1996), which included the additional information on precipitation (figure 6a), seems to work almost similar to the model of Kawai and Kawamura, which does not include the information on precipitation (figure 6b). For both models, the errors are low when the ΔSSTs are low (say less than 1.0°C) and are higher when the ΔSSTs are higher. Hence, the model that includes precipitation does not seem to perform better than the model that depends only on wind speed and solar radiation.

To further test the effect of precipitation on Webster *et al* (1996) model, we have re-estimated the regression coefficients of equation (1) by excluding the precipitation term (table 5). The RMSE and mean remains unchanged. Similarly, the plots of differences between observed and estimated *vs.* ΔSST also remains unchanged (figure 7). As it can be seen from table 5, the coefficient associated with $\log(U)$ term only showed appreciable change, when the precipitation term (P) was excluded from equation (1). It may be noted that the Webster *et al* (1996) model was devised to estimate the ΔSST_{skin}, whereas we have used the model to estimate the ΔSST at a depth of 0.92 m. That could be a reason for the ineffectiveness of precipitation term in equation (1).

The Kawai and Kawamura (2002) model was also applied on the data from TRITON and RAMA buoys moored in the EIO. The differences between the observed and estimated ΔSSTs were similar to that at WHOI mooring in the AS (figure 6c). In the EIO also, the differences between the observed and estimated ΔSST were higher when ΔSST exceeded 1.0°C. The plots of ΔSST *vs.* wind speed (figure 8a) and ΔSST *vs.* solar radiation (figure 8b) show that the higher ΔSSTs (>1.0°C) are associated with low wind speeds and high solar radiation that mostly occurred in

Table 5. *Regression coefficients estimated for Webster et al (1996) model. The coefficients were estimated by including and excluding the precipitation term (P) in equation (1). Data from WHOI mooring was used.*

Precipitation term (P)	a	b	c	d	e	f	RMSE	Mean
Included	3.343×10^{-3}	-2.750×10^{-1}	3.352×10^{-1}	-1.562×10^{-3}	1.188×10^{-1}	-1.634	0.1940	-0.0400
Excluded	3.334×10^{-3}	0.00×10^{-1}	3.296×10^{-1}	-1.559×10^{-3}	1.196×10^{-1}	-1.626	0.1937	-0.0396

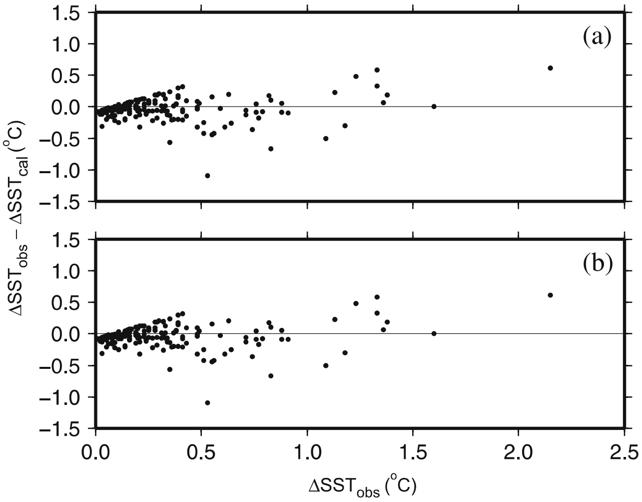

Figure 7. The errors in the estimation of ΔSST using the regression model proposed by Webster *et al* 1996 (equation 1). To assess the impact of precipitation on the estimation of ΔSST, the regression coefficients were estimated by including and excluding the precipitation term in equation 1. **(a)** the errors in ΔSST by including the precipitation term and **(b)** the errors in ΔSST by excluding the precipitation term.

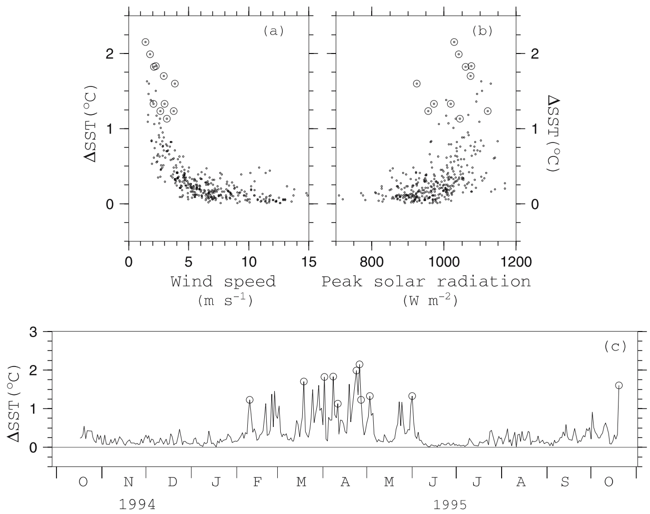

Figure 8. Relationships between **(a)** ΔSST and average wind speed during 04:00–16:00 LST, **(b)** ΔSST and peak solar radiation during a day and **(c)** the time series of ΔSST. Data is from WHOI mooring for the period during 15 October 1994 to 15 October 1995. The data points yielding higher error ($>1.0°$C) are identified with circles.

spring (figure 8c). A larger dataset covering varying atmospheric conditions is necessary to analyse the reasons behind comparatively bad performance of the model under low winds and high solar radiation. In the absence of such dataset for the north Indian Ocean region, we have attempted the analysis of this problem using WHOI data and a 1-D heat balance model.

Ignoring the effects of oceanic advection, diffusion, mixing, etc., in the heat balance for the upper most 2.0 m layer of the water column at a location can be written as:

$$\rho_w H C_p \frac{\partial T}{\partial t} = (1-\beta)R_s + R_l + Q_l + Q_s, \qquad (3)$$

where T is the mean temperature in the H m layer of the water column (2.0 m); $\rho_w = 1026.0\,\mathrm{kg\ m^{-3}}$ is the mean density of sea water in that water column and $C_p = 3902\,\mathrm{J\ kg^{-1}K^{-1}}$ is the specific heat of water. R_s, R_l, Q_l and Q_s represent the net short wave radiation, net long wave radiation, latent heat flux and sensible heat flux. The latent and sensible heat fluxes are directly proportional to the magnitude of wind speed. β represents the fraction of R_s that penetrates and escapes the 2.0 m water column. For this analysis, $\beta = 0.58$ was used following Jerlov (1976).

Figure 9 shows the plots of terms on the LHS and RHS of equation (3) and the wind speed. In spring, the large variability in the LHS of equation have caused higher mismatch between the two sides of equation (3) (figure 9a). This would mean that the large warming rates in spring (LHS) are not in balance with the net effect of the terms on RHS. Perhaps, the processes not considered in this 1-D model, such as oceanic advection, diffusion and mixing are necessary to account for the large fluctuations in the rate of warming in spring. This could be the reason for the bad performance of equation (2) that uses only wind speed and short wave radiation to estimate ΔSST.

4. Summary and conclusions

The purpose of this study was to describe the variability in the magnitudes of diurnal ranges of SST

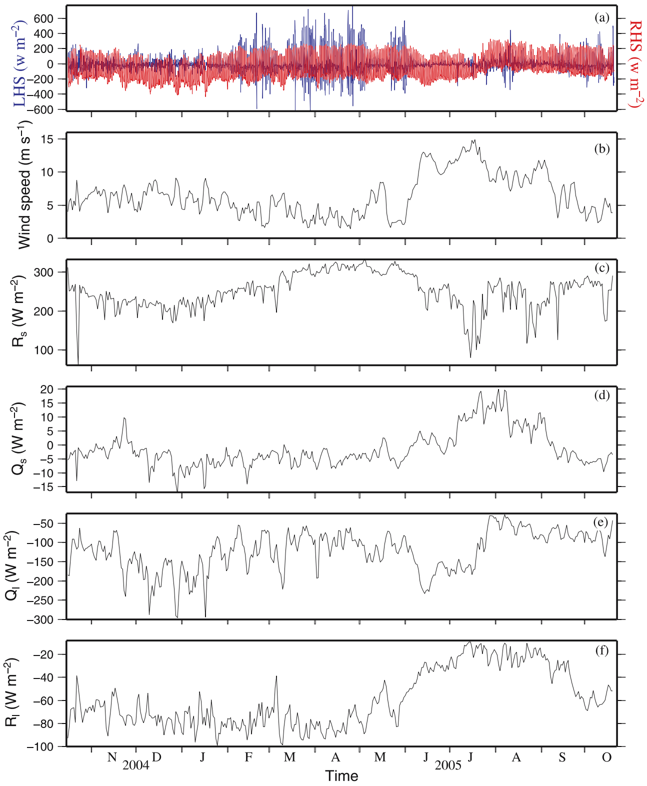

Figure 9. Time series of the terms on the LHS ($\rho_w H C_p(\partial T/\partial t)$) and RHS ($(1-\beta)R_s + R_l + Q_l + Q_s$) of 1-D heat balance equation (equation 3). See text for the explanations of symbols used. Time series of wind speed is also shown. Data is from WHOI mooring for the period during 15 October 1994 to 15 October 1995.

over the north Indian Ocean using *in situ* measurements and to examine the suitability of simple regression models for the estimation of diurnal SST ranges. *In situ* measurements obtained from 1556 drifting and 25 moored buoys were used to estimate the magnitudes of diurnal range of SST in the north Indian Ocean. The analysis showed the high seasonality in the magnitudes of diurnal range of SST (ΔSST) over the north Indian Ocean. About 80% of the observed ΔSST values were lower than 0.5°C during summer and winter monsoons. During the inter-monsoon months (May and October) 70% of the ΔSSTs were below 0.5°C. Lowest percentage of cooler ΔSST (<0.5°C) occurred in spring. During spring, about 45% of the ΔSST values were higher than 0.5°C. During the summer monsoon, only 8–10% observations exceeded 1.0°C. The seasonality in the diurnal warming is due to the seasonality associated with the strength of surface winds and the solar radiation received at the surface. During the summer monsoon, over the north Indian Ocean, the winds are strong and the cloudy skies supress the solar radiation arriving at the surface. Both of these factors favour the reduction of ΔSST. On the other hand, during spring, the winds are weaker and the solar radiation is higher due to the absence of clouds. Both of these factors promote large diurnal warming.

Except for the seasonality in the magnitudes of ΔSST amplitude, the spatial variability across the three segments of the north Indian Ocean (AS, BB, EIO) basin does not differ significantly except during the winter monsoon and in May. During the winter monsoon, the variability in the magnitudes of ΔSST in the AS differed significantly with that in the BB. Similarly, in May, the distribution of ΔSST in the AS differed with BB as well as with EIO (table 3).

The simple regression model (Kawai and Kawamura 2002) based on average wind speed and peak solar radiation is good enough to estimate the ΔSST amplitude, though the errors are higher at the higher magnitudes of ΔSST (>1.0°C) that occurred under low wind high solar radiation conditions. The additional information on precipitation as suggested in the model of Webster *et al* (1996) seems to be redundant in improving the accuracy of ΔSST estimates obtained using the temperature measurements at around 1.0 m depth.

The observations presented here are important for modelling the intraseasonal amplitude of SST (Shinoda and Hendon 1998) and phytoplankton biomass in the Arabian Sea (McCreary *et al* 2001) because they provide an estimate of the magnitude of diurnal warming and its seasonality in the north Indian Ocean. The modelling studies of Bernie *et al* (2007) showed the importance of diurnal cycle in the intraseasonal SST response to MJO. Similarly, the magnitude of diurnal warming has implications for the accuracy of SSTs retrieved using satellite based sensors. The expected error in the retrievals of SST using satellite based infrared sensor is 0.4°C (Shenoi 1999) and that using the microwave sensor is 0.6°C (Bhat *et al* 2004) in the north Indian Ocean. But the large magnitude of diurnal warming reported here will introduce larger errors in the retrieved SSTs, especially in spring.

Acknowledgements

The WHOI, RAMA and TRITON moored buoys data were obtained from http://kuvasz.whoi.edu/uopdata/arabiansea/arabianseamet.html, http://www.pmel.noaa.gov/tao/disdel/disdel.html and http://www.jamstec.go.jp/jamstec/TRITON/real_time/php/delivery.php, respectively. The NDBP moored buoy data was obtained from the data archives of NDBP/NIOT, Chennai. We are grateful to GDC/AOML/NOAA, Miami, USA for providing the drifter data. Financial support from Ministry of Earth Sciences, New Delhi, through

INCOIS, Hyderabad is acknowledged. The figures in this manuscript were prepared using GMT software. This is NIO contribution 4556.

References

Anderson T W 1962 On the distribution of the two-sample Cramer-von Mises criterion; *Ann. Math. Statist.* **33** 1148–1159.

Bernie D J, Guilyardi E, Madec G, Slingo J M and Woolnough S J 2007 Impact of resolving the diurnal cycle in an ocean-atmosphere GCM. Part 1: a diurnally forced OGCM; *Clim. Dyn.* **29** 575–590.

Bhat G S, Vecchi G A and Gadgil S 2004 Sea surface temperature of the Bay of Bengal derived from TRMM Microwave Imager; *J. Atmos. Ocean Tech.* **21** 1283–1290.

Clayson C A and Chen A 2002 Sensitivity of a coupled single-column model in the Tropics to treatment of the interfacial parameterizations; *J. Clim.* **15** 1805–1831.

Clayson C A and Weitlich D 2007 Variability of tropical diurnal sea surface temperature; *J. Clim.* **20** 334–352.

Cornillon P and Stramma L 1985 The distribution of diurnal sea surface warming events in the western Sargasso Sea; *J. Geophys. Res.* **90** 11,811–11,815.

Donlon C J and the GHRSST-PP Science Team 2005 The recommended GHRSST-PP data processing specification GDS (version 1 revision 1.6). The GHRSST-PP international project office, Exeter, UK, 245 pp. (available at http://ghrsst-pp.jrc.it/documents/GDS-v1.6.zip).

Fairall C W, Bradley E F, Godfrey J S, Wick G A, Edson J B and Young G S 1996 Cool-skin and warm layer effects on sea surface temperature; *J. Geophys. Res.* **101** 1295–1308.

Gentemann C L, Donlon C J, Stuart–Menteth A and Wentz F J 2003 Diurnal signals in satellite sea surface temperature measurements; *Geophys. Res. Lett.* **30** L1140 doi: 10.1029/2002GL016291.

Hansen D V and Poulain P-M 1996 Quality control and interpolations of WOCE-TOGA drifter data; *J. Atmos. Oceanic Technol.* **13** 900–909.

Jerlov N G 1976 Marine Optics; *Elseveir Oceanography Series* **14** 231 pp.

Kawai Y and Kawamura H 2002 Evaluation of the diurnal warming of sea surface temperature using satellite-derived marine meteorological data; *J. Oceanogr.* **58** 805–814.

Kawai Y and Wada A 2007 Diurnal sea surface temperature variation and its impact on the atmosphere and ocean: A review; *J. Oceanogr.* **63** 721–744.

Kennedy J J, Brohan P and Tett S F B 2007 A global climatology of the diurnal variations in sea-surface temperature and implications for MSU temperature trends; *Geophys. Res. Lett.* **34** L05712 doi: 10.1029/2006GL028920.

McCreary J P, Kohler K E, Hood R R, Smith S, Kindle J, Fischer A S and Weller R A 2001 Influences of diurnal and intraseasonal forcing on mixed-layer and biological variability in the central Arabian Sea; *J. Geophys. Res.* **106** 7139–7155.

Minnett P J 2003 Radiometric measurements of the sea-surface skin temperature – the competing roles of the diurnal thermocline and the cool skin; *Int. J. Remote Sens.* **24** 5033–5047.

Price J F, Weller R A and Pinkel R 1986 Diurnal cycling: observations and models of the upper ocean response to diurnal heating, cooling and wind mixing; *J. Geophys. Res.* **91** 8411–8427.

Price J F, Weller R A, Bowers C M and Briscoe M G 1987 Diurnal response of sea-surface temperature observed at the long-term upper ocean study (34 N, 70 W) in the Sargasso Sea; *J. Geophys. Res.* **92** 14,480–14,490.

Shinoda T 2005 Impact of the diurnal cycle of solar radiation on intraseasonal SST variability in the western equatorial Pacific; *J. Clim.* **18** 2628–2636.

Shinoda T and Hendon H H 1998 Mixed layer modeling of intraseasonal variability in the tropical western Pacific and Indian Oceans; *J. Clim.* **11** 2668–2685.

Shenoi S S C 1999 On the suitability of global algorithms for the retrieval of SST from the North Indian Ocean using NOAA/AVHRR data; *Int. J. Remote Sens.* **20** 11–29.

Solomon A and Jin F-F 2005 A study of the impact of off-equatorial warm pool SST anomalies on ENSO cycles; *J. Clim.* **18** 274–286.

Sreejith O P and Shenoi S S C 2002 An evaluation of satellite and *in situ* based sea surface temperature data sets in the North Indian Ocean region; *Int. J. Remote Sens.* **23** 5165–5175.

Stramma L, Cornillon P, Weller R A, Price J F and Briscoe M G 1986 Large diurnal sea surface temperature variability: Satellite and *in situ* measurements; *J. Phys. Oceanogr.* **16** 345–358.

Stuart–Menteth A C, Robinson I S and Challenor P G 2003 A global study of diurnal warming using satellite-derived sea surface temperature; *J. Geophys. Res.* **108** C3155.

Webster P J, Clayson C A and Curry J A 1996 Clouds, radiation and the diurnal cycle of sea-surface temperature in the tropical western Pacific; *J. Clim.* **9** 1712–1730.

Weller R A, Baumgartner M F, Josey S A, Fischer A S and Kindle J C 1998 Atmospheric forcing in the Arabian Sea during 1994–1995: Observations and comparisons with climatology and models; *Deep-Sea Res. Part II* **45** 1961–1999.

Weller R A, Fischer A S, Rudnick D L, Erickson C C, Dickey T D, Marra J, Fox C and Leben R 2002 Moored observations of upper-ocean response to the monsoons in the Arabian Sea during 1994–1995; *Deep-Sea Res. Part II* **49** 2195–2230.

Yokoyama R, Tanba S and Souma T 1995 Sea surface effects on the sea surface temperature estimation by remote sensing; *Int. J. Remote Sens.* **16** 227–238.

Zeng X, Zhao M, Dickinson R E and He Y 1999 A multiyear hourly sea surface skin temperature data set derived from the TOGA TAO bulk temperature and wind speed over the tropical Pacific; *J. Geophys. Res.* **104** 1525–1536.

MS received 18 August 2008; revised 15 April 2009; accepted 4 May 2009